Crystal Structure of a Catalytic Antibody with a Serine Protease Active Site

G. Wayne Zhou, Jincan Guo, Wei Huang, Robert J. Fletterick,* Thomas S. Scanlan*

The three-dimensional structure of an unusually active hydrolytic antibody with a phosphonate transition state analog (hapten) bound to the active site has been solved to 2.5 Å resolution. The antibody (17E8) catalyzes the hydrolysis of norleucine and methionine phenyl esters and is selective for amino acid esters that have the natural α-carbon L configuration. A plot of the pH-dependence of the antibody-catalyzed reaction is bell-shaped with an activity maximum at pH 9.5; experiments on mechanism lend support to the formation of a covalent acyl-antibody intermediate. The structural and kinetic data are complementary and support a hydrolytic mechanism for the antibody that is remarkably similar to that of the serine proteases. The antibody active site contains a Ser-His dyad structure proximal to the phosphorous atom of the bound hapten that resembles two of the three components of the Ser-His-Asp catalytic triad of serine proteases. The antibody active site also contains a Lys residue to stabilize oxyanion formation, and a hydrophobic binding pocket for specific substrate recognition of norleucine and methionine side chains. The structure identifies active site residues that mediate catalysis and suggests specific mutations that may improve the catalytic efficiency of the antibody. This high resolution structure of a catalytic antibody-hapten complex shows that antibodies can converge on active site structures that have arisen through natural enzyme evolution.

Enzymes have evolved precise structures that enable them to catalyze chemical reactions with exquisite efficiency. An active goal of research in protein engineering is the creation of novel catalysts with the high levels of activity and specificity of natural enzymes. One approach is to change the natural substrate specificity of an enzyme through mutagenesis. The substrate specificities of aspartate aminotransferase (*1*), lipoxygenase (*2*), and the serine proteases trypsin (*3*), α-lytic protease (*4*), and subtilisin (*5*) have been successfully altered where this approach was used without destroying the catalytic activity of the enzyme. Because binding specificity and catalytic activity may be inextricably linked in enzymes, however, it is not always possible to predict how an active site mutation might affect catalytic activity.

An alternative approach is the induction of catalytic activity in antibodies, which are singularly adaptable binding proteins that have broad and programmable ligand specificity. An impressive array of chemical reactions has been shown to be subject to antibody catalysis demonstrating the generality of this approach (*6*). In addition, because substrate specificity can be precisely programmed in catalytic antibodies through antigen design, catalytic antibodies often show higher substrate discrimination than analogous enzymes. Turnover numbers (k_{cat}) for catalytic antibodies range from low values to values that approach those of enzymes. However, the structural basis for the high turnover numbers observed for some catalytic antibodies is not well understood.

Structural studies of catalytic antibodies are essential for defining the limits of catalytic activity that can be achieved with antibodies. Catalytic antibodies with higher activity might contain active site residues that resemble the highly efficient active site chemistry of enzymes. To date, only two three-dimensional structures of catalytic antibodies with bound haptens have been reported (*7*); one is the phosphorylcholine-specific antibody MCPC603 (*8*) expressed by myeloma cells, which exhibits hydrolytic activity with choline carbonates (*9*), and the other for an antibody to a transition state analog that shows chorismate mutase activity (*10*). We now describe the three-dimensional structure of a catalytic antibody with unusually high esterolytic activity. The structural arrangement of active site residues and the kinetic data support a catalytic mechanism for the antibody that is similar to that used by serine proteases.

Kinetic and mechanistic studies. We have reported the generation and kinetic characterization of the antibody 17E8, which was raised to a norleucine-phosphonate transition state analog **4** (Fig. 1A) and catalyzes the hydrolysis of norleucine and methionine phenyl esters (**1** and **2**) (*11*). Phosphonates were originally proposed as haptens for hydrolytic antibodies because it was expected that they would induce combining site structures that stabilize the energetically unfavorable interactions of the rate-limiting hydrolysis transition state (*12*, *13*). The steady-state kinetic constants for 17E8-catalyzed ester hydrolysis compare favorably to other hydrolytic antibodies (*6*): the maximum k_{cat} for 17E8 is 223 min^{-1} and the maximum rate acceleration (k_{cat}/k_{uncat}) is 2.2×10^4 (*14*). Hydrolysis is enantioselective for amino acid esters with the natural *S*(L) configuration at the α-carbon; ester substrates with the *R*(D) configuration at the α-carbon were not processed.

The antibody-catalyzed hydrolysis reaction gave a bell-shaped pH-rate profile (Fig. 1B) suggesting that two ionizable residues with p*K*a's of 9.1 and 10.0 in the 17E8 active site could mediate hydrolysis. Maximum activity for 17E8 is achieved at pH 9.5 where the p*K*a 9.1 residue is deprotonated and the p*K*a 10.0 residue is protonated. An acyl-antibody intermediate was detected in mechanistic experiments and the rate-limiting step in catalysis was defined as formation of the intermediate (*15*). Bell-shaped pH-rate profiles and acyl intermediate formation are characteristic of enzymatic hydrolysis mechanisms for active site residues that function as nucleophiles, general acids, and general bases.

Crystallization, data collection, and structure analyses. The antibody binding (Fab) fragment of 17E8 was prepared from the full-length 17E8 immunoglobulin by standard technique (*16*). The purified Fab was concentrated to 14 mg/ml in 10 mM tris, pH 7.5, and 0.01 percent NaN_3, and combined with 1 to 1.5 molar equivalents of hapten **4** used as a racemic mixture. The crystallization screen for the complex was set up in hanging drops for the factorial screening method (*17*). Small crystals were observed on the second day. The optimal crystallization conditions were refined by trial and error until crystals of about 0.2 mm^3 could be obtained reproducibly. The crystal used for data collection was grown in a reservoir containing 0.1M hepes, pH 7.5, 15 percent polyethylene glycol (PEG-4K), and 5 percent isopropanol. In the hanging drop, 2 μl of protein (14 mg/ml) with hapten **4** at 4.5 mM (1.5 molar ratio to protein) were combined in a 4-μl reservoir solution. Satisfactory crystals were obtained from this drop in 1 week at room temperature.

A 2.5 Å x-ray data set was measured at room temperature on a Siemens area detec-

G. W. Zhou and R. J. Fletterick are in the Department of Biochemistry and Biophysics and Department of Pharmaceutical Chemistry, University of California, San Francisco, CA 94143–0448, USA. J. Guo, W. Huang, and T. S. Scanlan are in the Department of Pharmaceutical Chemistry, University of California, San Francisco, CA 94143–0446, USA.

*To whom correspondence should be addressed.

tor (50 kV and 60 mA) from a crystal with dimensions of 0.2 by 0.2 by 0.1 mm^3. The space group was expected to be either $P2$ or $P2_1$. This ambiguity was resolved by the translation function search. The unit cell lengths are $a = 41.41$ Å, $b = 78.06$ Å, $c = 81.94$ Å, $\beta = 94.94°$ (Table 1).

The structure of the 17E8 Fab-hapten complex was determined to 2.5 Å resolution by molecular replacement. The arsenate-specific antibody 1fai (R19.92) was used as an initial model for molecular replacement because it belongs to the same isotype subgroup (IgG2b,κ) as 17E8 (*18*). The sequence identity between 17E8 and 1fai is 84 percent. A modified 1fai coordinate set was used as a search model; all residues that represented deletions (L 95, and H 105 to H 109; L, light chain; H, heavy chain) in 17E8 relative to 1fai were omitted, and all nonidentical amino acids were truncated to alanine, except when the amino acid was a glycine in 17E8. The X-PLOR program package (*19*, *20*) was used for the rotation search, Patterson correlation (PC) refinement, and translation search (*21*).

An electron density map based on coefficients of $2F_o-F_c$ was calculated from the phases of the initial model. Amino acid side chains were built and placed in visible density. The gap between residues 94 and 96 of the light chain of the antibody was closed according to the density. Because of the five deletions, the CDR3 region of the heavy chain (residues 98–113) was deleted from the second cycle model and amino acids were then added and modified one by one during the next 17 cycles of slow-cooling and conjugate gradient refinement. This sequence resulted in an R factor of 0.199 with root mean square (rms) differences of 0.37 and 0.34 Å for the variable domains of the light and heavy chains, respectively.

Significant density was observed at the hapten binding site in the $2F_o-F_c$ map. Models of both R(L) and S(D) enantiomers of hapten **4** were generated by the program Insight II. Only the R enantiomer fit the electron density of **4**. Topology and parameter files dictating the chemical structure and bonding characteristics of the hapten were prepared for X-PLOR. Three additional cycles of "slow-cool" refinement and model adjustment were performed, resulting in a final R factor of 18.6 percent with rms deviations of bond lengths and bond angles from ideality of 0.011 Å and 3.097°, respectively. The electron density, shows the orientation of the side chains of both protein and hapten **4** (Fig. 2).

The 17E8 Fab structure shows overall similarity to other known antibody structures (Fig. 3) (*22*). The light and heavy chain variable domains (without the CDR3 regions) can be superimposed on the vari-

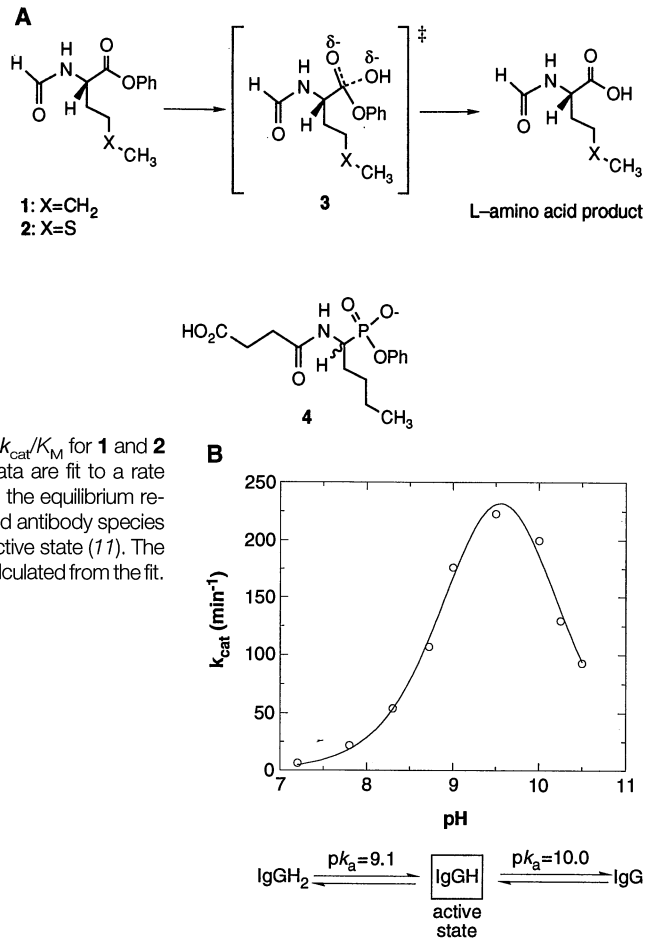

Fig. 1. (**A**) Amino acid ester hydrolysis reaction catalyzed by antibody 17E8 and structure of norleucine phosphonate hapten (**4**) used to elicit the antibody 17E8. The hapten is designed to mimic the transition state (**3**) leading to the tetrahedral hydrolysis intermediate. The antibody catalyzes the hydrolysis of both norleucine (**1**) and methionine (**2**) phenyl esters. (**B**) The pH rate profile for 17E8-catalyzed hydrolysis of the norleucine phenyl ester **1**; the methionine ester **2** gives a similar pH rate profile. Plots of k_{cat}/K_M for **1** and **2** are similarly bell-shaped. The data are fit to a rate equation (r=0.995) derived from the equilibrium relation where the singly protonated antibody species (IgGH) is the most catalytically active state (*11*). The pK_a values of 9.1 and 10.0 are calculated from the fit.

Table 1. Summary of data collection and refinement statistics.

Crystal and diffraction data			
Space group	$P2_1$		
Cell dimensions	a = 41.41, b = 78.06, c = 81.94, β = 94.94°		
Resolution (Å)	2.5*		
Total reflections	34,177		
Unique reflections	13,531		
R_{merge}	0.076		
Structure determination by molecular replacement			
Search model:			
1fai, Fab fragment from the arsonate-specific monoclonal antibody, R19.92 (IgG2b, κ)			
light chain	214 amino acids	1 deletion	33 mutations
heavy chain	221 amino acids	5 deletions	34 mutations
Sequence Identity 84 percent			
X-PLOR refinement			
R_{cryst}	0.186		
Resolution (Å)	6.0–2.5		
rms differences			
Bond (Å)	0.011		
Angle (deg)	3.087		

*Fifty percent of the data from 2.75 to 2.5 Å are better than 1σ, and 75 percent of the data from 15 to 2.5 Å are observed.

Table 2. Atomic contacts between the bound hapten and the active site of 17E8.

Atom 1	Atom 2	Distance (Å)
P (**4**)	Cβ Ser^{H99}	4.2
P (**4**)	Oγ Ser^{H99}	5.6
		3.0*
O (pro-S, **4**)	Nζ Lys^{H97}	2.5
P (**4**)	Nε His^{H35}	4.1
Oζ Tyr^{H101}	Oγ Ser^{H99}	3.0
H-Oζ Tyr^{H101}	Oγ Ser^{H99}	2.0
Nε His^{H35}	Oγ Ser^{H99}	2.7†

*This distance is measured after a 180° rotation about Cα-Cβ of the side chain of Ser^{H99}. †This distance is measured after the side chain of His^{H35} is rotated 45° about Cα–Cβ and 60° about Cβ–Cγ bond with Ser^{H99} rotated 180° as described.

able domains of 1fai with rms values of 0.84 Å and 0.73 Å for the common Cα carbons (from Insight II). The CDR3 loop of the 17E8 light chain is shortened by one amino acid. The CDR3 loop of the heavy chain is shortened by five amino acids, and the loop is narrowed and moved away from the CDR3 of the light chain. The hapten **4** is bound in a deep cleft between the light and heavy chain CDR3. The carboxylate group of **4**, used as an attachment site to carrier protein, lies at the entrance of the cleft and is surrounded by five tyrosines (L50, H32, H50, H92, and H101). There are six hydrogen bonds and van der Waals contacts with 31 atoms of 14 amino acids between **4** and the antibody. The phenyl ring of **4** is bound in a hydrophobic pocket formed by the side chains of Leu^{L89}, Tyr^{L36}, Trp^{H47}, Arg^{L96}, with Val^{H37} and Phe^{L98} at the bottom of the pocket (Fig. 4).

Examination of the combining site structure of 17E8 shows that recognition of the hydrophobic side chain of **4** is mediated by light chain residues, and recognition of the anionic phosphonate group of **4** is mediated predominantly by heavy chain residues. These separate recognition sites reside on opposite sides of the 17E8 binding cleft. A pocket containing the side chains (and backbone) of three light chain residues Leu^{L89}, Gly^{L34}, and Tyr^{L91} forms a hydrophobic binding site for the *n*-butyl (norleucine) side chain of **4** (Fig. 4). Recognition of the phosphonate oxyanion of **4** is mediated by the ε-amino of Lys^{H97} through a salt bridge contact to the pro-*S* oxygen of **4** (Fig. 5A), and a potential hydrogen bonding interaction between Arg^{L96} and the pro-*R* oxygen of **4**. Other amino acid side chains that are within 6.0 Å of the phosphorous atom of **4** reside in CDR1 and CDR3 of the heavy chain include Ser^{H99}, Tyr^{H101}, and His^{H35} (Table 2).

The structure of the 17E8-**4** complex shows the L-enantiomer of phosphonate **4** bound to the active site even though a racemic mixture of hapten **4** was used in the crystallization experiment (Fig. 5A). The combining site of 17E8 is thus specific for one of the two enantiomers of phosphonate **4**. This hapten-binding selectivity correlates with the L-enantioselectivity of the antibody-catalyzed hydrolysis reaction. Because the active site of 17E8 is complementary to the L-phosphonate enantiomer, the antibody is able to bind and hydrolyze only amino acid esters that bear the natural α-carbon configuration.

Hydrolytic mechanism. A mechanism for 17E8 hydrolysis that is consistent with our kinetic and structural data is similar to the hydrolytic mechanism of serine proteases (*23*). These enzymes catalyze the hydrolysis of both amide and ester substrates through a covalent ester intermediate that is formed between the acyl portion of the substrate and an active site serine residue of the enzyme. The nucleophilicity of the active site serine residue is enhanced by interactions from neighboring histidine and aspartate residues. The stereoelectronic features of this triad result in the activation of a high pK_a serine hydroxyl group at physiological pH. This active site Ser-His-Asp catalytic triad is conserved in all serine proteases and is largely responsible for the enormous rate accererations displayed by this family of enzymes.

The pH-rate studies on 17E8-catalyzed ester hydrolysis suggest that a protonated residue with a pK_a of 10.0 accelerates hydrolysis. This pK_a is in the range of a lysine ε-amino group (*24*); that the rate of hydrolysis decreases at pH values where this

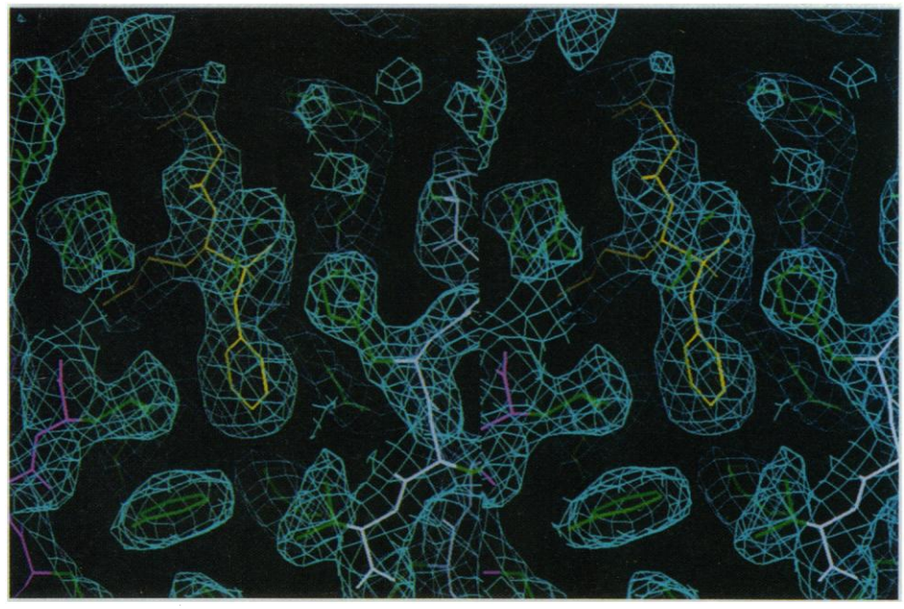

Fig. 2. The $2F_o-F_c$ density map of the hapten binding site. The hapten (**4**) is shown in yellow, the backbones of the light chain and heavy chain are shown in pink and white respectively, and the side chains are shown in green. The density map is contoured at 1σ and shown in cyan.

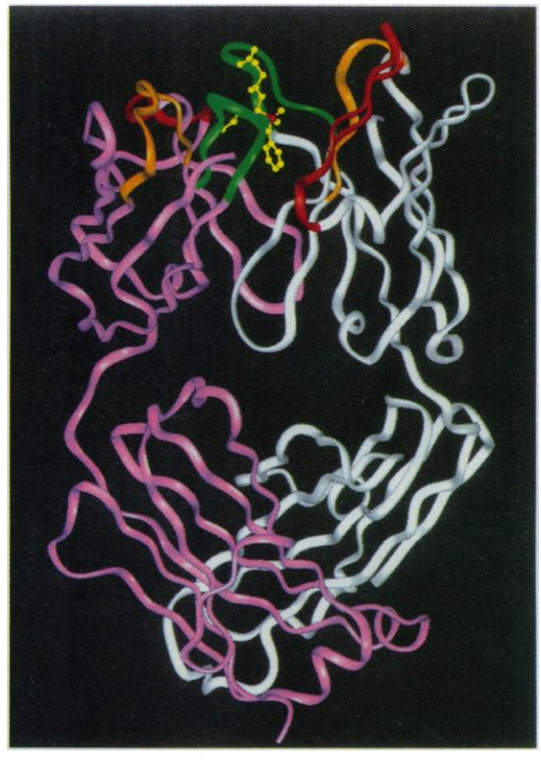

Fig. 3. A ribbon diagram of the 17E8 Fab fragment with bound hapten **4**. The light chain is shown in pink, and the heavy chain is shown in white. The CDR regions in both domains are colored as orange, red, and green for 1, 2, and 3 respectively. The hapten **4** is shown in yellow, as a ball-and-stick model. The phosphorous atom of **4** is shown in red. The V domains of both the light chain and heavy chain of 17E8 are superimposable to those of the search model, 1fai. The light chain CDR3 of 17E8 is one amino acid shorter than that of the search model. The heavy chain CDR3 of 17E8 is quite different from the search model. Five amino acids are deleted in the top of CDR3, the loop has been narrowed (between residues 99 and 111), and more space is available for hapten binding.

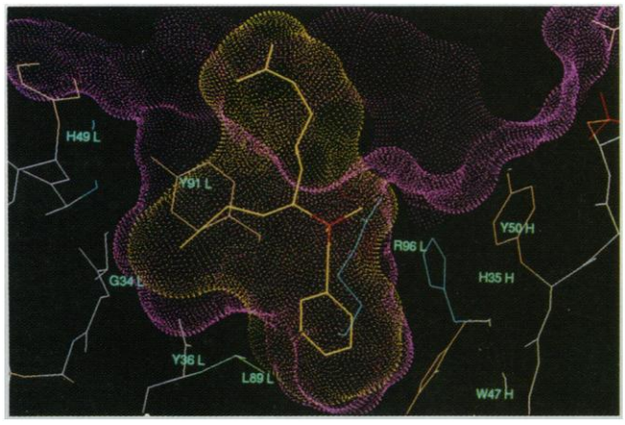

Fig. 4. The 17E8 binding pockets for the phenyl phosphonate and n-butyl side chain of hapten **4**. The solvent accessible surfaces of the hapten and antibody are shown in yellow and magenta respectively. The hapten is represented by bonds in yellow, with the phosphous atom in red. The backbone of the antibody is in white for the heavy chain and pink for the light chain, and the side chains are colored according to their polarity, red negative, cyan positive, green aliphatic, brown aromatic. The diagram shows a good fit between the surface of the hapten and the surface of the binding pocket. The phenyl phosphonate binding pocket is composed of side chains from Leu^{L89}, Tyr^{L36}, Trp^{H47}, Arg^{L96}, with Val^{H37} and Phe^{L98} at the bottom. The binding pocket for the *n*-butyl side chain is formed exclusively from the light chain residues Leu^{L89}, Gly^{L34}, Tyr^{L91}, and His^{L49}.

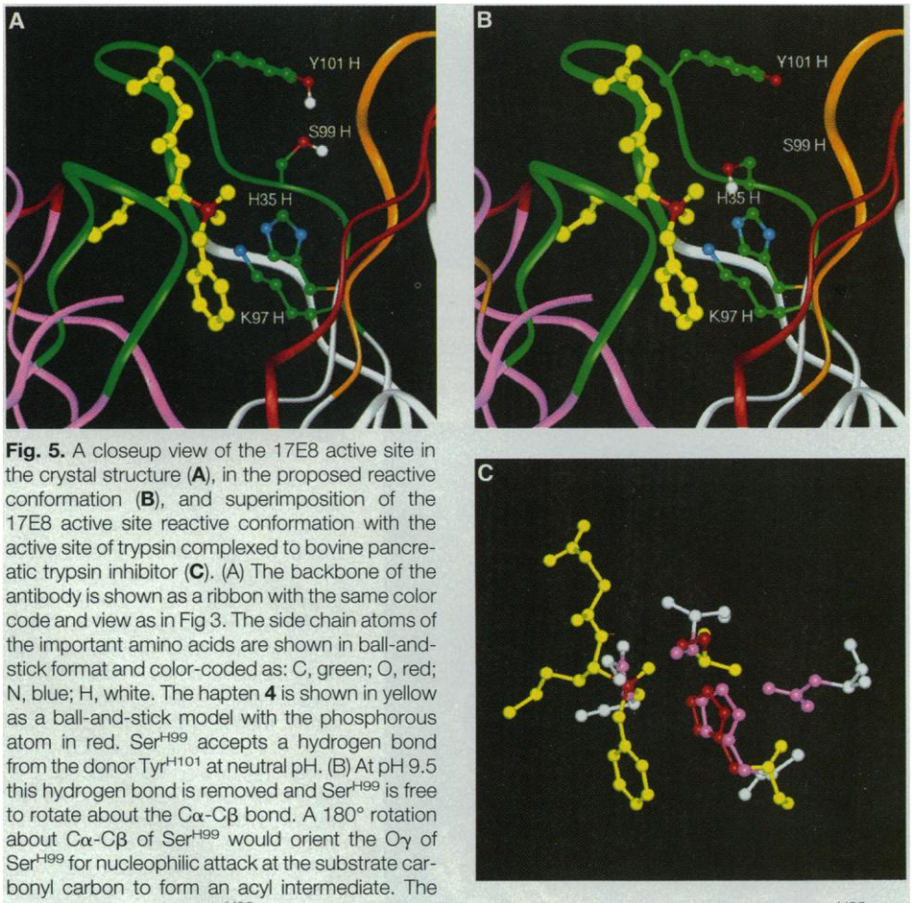

Fig. 5. A closeup view of the 17E8 active site in the crystal structure (**A**), in the proposed reactive conformation (**B**), and superimposition of the 17E8 active site reactive conformation with the active site of trypsin complexed to bovine pancreatic trypsin inhibitor (**C**). (A) The backbone of the antibody is shown as a ribbon with the same color code and view as in Fig 3. The side chain atoms of the important amino acids are shown in ball-and-stick format and color-coded as: C, green; O, red; N, blue; H, white. The hapten **4** is shown in yellow as a ball-and-stick model with the phosphorous atom in red. Ser^{H99} accepts a hydrogen bond from the donor Tyr^{H101} at neutral pH. (B) At pH 9.5 this hydrogen bond is removed and Ser^{H99} is free to rotate about the Cα-Cβ bond. A 180° rotation about Cα-Cβ of Ser^{H99} would orient the Oγ of Ser^{H99} for nucleophilic attack at the substrate carbonyl carbon to form an acyl intermediate. The nucleophilicity of the Ser^{H99} hydroxyl would be enhanced by a hydrogen bond to the Nε of His^{H35} (see Table 2). The Nε of Lys^{H97} resides on the opposite face of the substrate carbonyl and functions electrostatically to stabilize the developing negative charge at the carbonyl oxygen. (C) Superimposition of the active site reactive conformation of 17E8 and the active site structure of trypsin complexed with BPTI. The catalytic residues are on the right side with backbone and side chain atoms of trypsin in white and pink, respectively, and backbone and the side chain atoms of 17E8 in yellow and red, respectively. The trypsin active site contains a Ser-His-Asp catalytic triad whereas the catalytic antibody active site contains a Ser-His catalytic dyad. On the left side, backbone residues 15-16 of BPTI are shown in white, with the C and N atoms of the amide bond between residues 15 and 16 shown in pink. The phosphonate hapten **4** superimposed with the BPTI structure is shown in yellow with the phosphorous atom in red.

group is largely deprotonated suggests that the protonated ε-amino functions as a cationic component that stabilizes the developing oxyanion in the transition state. The active site structure of 17E8 shows the ε-amino group of Lys^{H97} positioned 2.5 Å from the pro-S phosphonate oxygen of **4** (Fig. 5A). This structural relation supports the assignment of Lys^{H97} as an analog of an oxyanion hole. If **4** is an accurate mimic of the hydrolysis transition state, this structure suggests that the incoming nucleophile attacks from the re-face of the substrate carbonyl as in the serine proteases and occupies the position of the pro-*R* oxygen of **4** in the transition state.

Our mechanistic studies support the rate-limiting formation of a covalent acyl-intermediate in 17E8-catalyzed ester hydrolysis. If this intermediate is an acyl-antibody species analogous to the acyl-enzyme intermediate seen with serine proteases, then an active site nucleophile should reside within the immediate vicinity of the phosphorous atom of **4**. The anion of a pK_a 9.1 residue in 17E8, in the range for a tyrosine hydroxyl (*24*), substantially accelerates hydrolysis (Fig. 1B). There are four tyrosine residues in the 17E8 active site although none is close enough to the phosphorous atom of **4** for direct nucleophilic attack and their hydroxyl groups do not interact with **4**. Tyr^{H101}, however, orients the hydroxyl group of Ser^{H99} away from **4** by a hydrogen bond (Fig. 5A). A 180° rotation about the Cα-Cβ bond of Ser^{H99} positions the hydroxyl about 3 Å from the phosphorous atom of **4** (Fig. 5B). This rotation will also place the Ser^{H99} hydroxyl within hydrogen bonding distance (2.7 Å) of His^{H35}.

An important question is whether Tyr^{H101} functions as a hydrogen bond donor or hydrogen bond acceptor with Ser^{H99}. Electronic and geometric considerations suggest that Ser^{H99} cannot be a donor. Modeling hydrogen atoms into both Tyr^{H101} and Ser^{H99} and examining all possible rotations about all side chain sigma bonds unequivocally shows that appropriate hydrogen bond distance and angles can be achieved only if Tyr^{H101} is the hydrogen bond donor and Ser^{H99} is the hydrogen bond acceptor (*25*). This is a case where the hydrogen bonding arrangement between two hydroxyl-containing residues that in principle can be both hydrogen bond donors and acceptors is asymmetric, and the donor-acceptor roles of Tyr^{H101} and Ser^{H99} cannot be reversed.

Because Tyr^{H101} functions as the hydrogen bond donor and Ser^{H99} as the hydrogen bond acceptor, ionization of Tyr^{H101} both eliminates the hydrogen bond and creates a repulsive interaction that could trigger rotation about the Ser^{H99} Cα-Cβ bond, which would move Ser^{H99} into hydrogen bonding distance with His^{H35} and into a reactive orientation for nucleophilic attack

at the re-face of the bound substrate carbonyl (Fig. 5B). Acylation of Ser^{H99} by the ester substrate would then occur to form a covalent acyl-antibody intermediate as the experimentally observed rate-limiting step in hydrolysis. Deacylation occurs in a rapid subsequent step and presumably involves re-face hydroxide attack on the acyl-antibody intermediate. In this mechanism, the tyrosine ionization (pK_a, 9.1) does not accelerate catalysis by direct participation as a nucleophile or general base, but functions as a pH-sensitive switch that immobilizes the nucleophilic in the "off" state and releases it in the "on" state.

Comparison of antibody and enzyme active sites. The active site of 17E8 is remarkably similar to the active sites of serine proteases such as trypsin (*26–29*). Both the antibody and the enzyme active sites contain a recognition pocket for specific binding of the P_1 side chain of the amino acid substrate. In addition, the active site of both the antibody and enzyme contain structures to stabilize the development of negative charge in the tetrahedral hydrolysis intermediate (oxyanion hole and Lys^{H97}), as well as a proximal histidine-activated serine residue that functions as a nucleophile to produce a covalent acyl-protein intermediate. The active site structural similarity between the 17E8-**4** complex and that of trypsin-BPTI (bovine pancreatic trypsin inhibitor) is evident in Fig. 5C where the active site Ser and His side chains and the central atoms of the bound inhibitors (P for **4** and C for BPTI) are superimposed. This analysis shows that although the backbones of the catalytic antibody and enzyme are quite different, the side chain functional groups and inhibitor atoms that correspond to the substrate carbonyl undergoing acylation converge to remarkably similar relative distances and geometries.

Despite the structural similarity, there are important differences between the catalytic antibody and enzyme active sites. First, serine proteases such as trypsin contain a catalytic triad which includes a buried aspartate residue that functions with the histidine to enhance the nucleophilicity of the serine hydroxyl by stabilizing the developing positive charge on the histidine imidazole. The antibody active site contains no equivalent structure to the buried aspartate. Second, the oxyanion hole of trypsin is made up of charge-neutral, conformationally restricted backbone NH atoms; the equivalent structure in the antibody consists of a conformationally mobile cationic lysine ϵ-amino group. A third difference between the antibody and enzyme structures is that the serine proteases usually contain two or more side-chain recognition pockets (...S_2S_1-$S_1'S_2'$...) for binding amino acid side chains on either side of the substrate scissle carbonyl (...P_2P_1-$P_1'P_2'$...), whereas the antibody only contains one site capable of binding hydrophobic P_1 norleucine and methionine side chains. The additional substrate binding sites in the serine proteases play an important role in both substrate recognition and catalytic turnover (*30*).

Table 3. Comparison of catalytic triad composition with turnover number.

Enzyme	Catalytic triad composition			Substrate*	k_{cat} (min^{-1})	Ref.
	Ser	His	Asp			
Trypsin	+	+	+	Z-GPR-SBn	2,900	(*34*)
Trypsin	+	+	+	Z-GPR-AMC	3,300	(*34*)
Subtilisin	+	+	+	suc-AAPF-PNA	2,640	(*33*)
Trypsin D102S/S214E†	+	+	+	Z-GPR-AMC	570	(*35*)
Subtilisin S24C/D32A	+	+	−	suc-AAPF-PNA	1.1	(*33*)
Trypsin D102N	+	+	−	Z-GPR-SBn	3.0	(*34*)
Catalytic antibody 17E8	+	+	−	for-Norleu-OPh (**1**)	223	(*11*)

*Substrates are all activated amide and oxy and thioester derivatives. Abbreviations: Z, benzyloxycarbonyl; SBn, thiobenzyl ester; AMC, 7-amido-4-methylcoumarin; suc, succinyl; PNA, *p*-nitroanilide; for, formyl. †This double mutant of trypsin contains a glutamate residue at a different location in protein that replaces Asp^{102} in the catalytic triad.

Site-directed mutagenesis experiments by others have demonstrated that the aspartate component of the catalytic triad of serine proteases plays a critical role in catalysis (*31–35*). The importance of the aspartate component of the catalytic triad in serine proteases can be seen by comparing the turnover numbers of serine protease mutants that lack the active site aspartate with those of the wild-type enzyme (Table 3) (*36*). These experiments show that mutations which replace the aspartate with residues devoid of the acidic side chain decrease the turnover number by a factor of 10^3 to 10^4. As has been demonstrated with trypsin, the high activity imparted by a complete catalytic triad can be substantially recovered when a glutamate residue is introduced into an alternative position in the protein backbone (trypsin D102S/214E, Table 3) (*35*). This result shows that the additional catalytic potency provided by the aspartate component of the triad can be largely compensated for by second-site mutations that place a carboxylate in the immediate vicinity of the active site histidine, and imply that the catalytic activity of our catalytic antibody may be substantially increased with the appropriate introduction of an aspartate or glutamate to complete the catalytic triad in the 17E8 active site.

It is important that the appearance of the Ser^{H99}–His^{H35} dyad in the active site of 17E8 is an unanticipated result of antibody variable region diversity and was not programmed from hapten design. None of the three residues that potentially participate in the hydrolytic mechanism (Tyr^{H101}, Ser^{H99}, and His^{H35}) appear to have significant interactions with the bound hapten **4**. Ser^{H99} and Tyr^{H101} appear to be partners in a hydrogen-bonding interaction that is important for structural reasons, possibly to enforce the geometry and relative position of the heavy chain CDR3. The only active site features of 17E8 that are the direct result of hapten design are the hydrophobic recognition pocket of the norleucine side chain and the oxyanion hole equivalent formed by the ϵ-amino of Lys^{H97}. It would be difficult to design a hapten structure that could reliably elicit these active site residues and induce a catalytic triad similar to that of a serine protease even though catalytic antibodies with these active site structures may exist in the immunoglobulin repertoire. The chances of isolating specifically active and potentially rare catalytic antibodies would be enhanced by new functional selection methods for probing the immunoglobulin repertoire that are based on catalytic activity rather than ligand binding (*37*, *38*).

The combination of a reasonably active first-generation catalytic antibody and a three-dimensional structure of the antibody-transition state analog complex presents an opportunity to introduce specific active site mutations that improve catalytic activity. For example, introducing an aspartate or glutamate residue to construct a full catalytic triad may lead to an improvement in activity for the reasons discussed above. Alternatively, a mutation that does not increase the k_{cat} of 17E8 directly but shifts the activity maximum from pH 9.5 to neutral pH would increase the catalytic efficiency (k_{cat}/k_{uncat}) of the antibody by 100 times because the uncatalyzed reaction is two orders of magnitude slower at pH 7.0 than at pH 9.5. The nucleophilic Ser^{H99} hydroxyl of 17E8 is held in an unreactive conformation through a hydrogen bond donated by Tyr^{H101}. We believe that removal of the Tyr^{H101} phenolic proton and disruption of this hydrogen bond is the pK_a 9.1 ionization that leads to a significant increase in hydrolytic activity (Fig. 1B). Changing Tyr^{H101} to phenylalanine would be a conservative mutation that would preserve the aromatic component of this residue yet remove this hydrogen bonding ability and po-

tentially shift the activity maximum toward neutral pH.

Alternatively, the active site chemistry of other families of protease enzymes could be explored with 17E8. For example, the active site of 17E8 also has similarity to the active site of thiol proteases such as papain, which have an active site Cys-His-Asn triad similar to the Ser^{H99}-His^{H35} dyad of 17E8 (39). The cysteine thiol is significantly more acidic than the serine hydroxyl, and the thiolate-imidazolium ion pair thought to be involved in the thiol protease hydrolytic mechanism provides a more potent nucleophile than a Ser-His hydrogen bonded pair (40–42). Mutation of Ser^{H99} to Cys would introduce a papain-like active site into 17E8 and, with the enhanced nucleophilicity, could provide a more active catalyst if formation of the acyl intermediate is the rate-limiting step in the antibody-catalyzed hydrolysis.

Catalytic antibodies and enzyme evolution. Catalytic antibody generation involves the introduction of catalytic activity into a protein structure that has evolved the natural function of ligand binding. Because they have not evolved natural enzymatic activity, catalytic antibodies provide an alternative protein framework for testing ideas of enzyme structure-function relations. Structural studies on unusually active catalytic antibodies like 17E8 may provide insight into the origins of the evolution of activity in natural enzymes. An important question is whether alternative catalytic strategies that are as effective as those used by modern enzymes may be discovered with catalytic antibodies. The structure of 17E8 shows that active site chemistry similar to that produced through natural enzyme evolution can also arise in the unnatural process of catalytic antibody generation. This structural convergence between the antibody and enzyme is interesting in that the active site structures of present-day serine proteases presumably arose from hundreds of millions of years of protein evolution whereas the active site of 17E8 was produced in a standard 50-day immunization schedule. The 17E8 active site may in a crude sense resemble the active site of an intermediate enzyme in serine protease evolution that lacks the third important asparate component of the catalytic triad. The close structural similarity between the antibody and enzyme active sites suggests that there may be relatively few mechanistic pathways for effective hydrolytic catalysis with protein frameworks made up of the natural amino acids, and that the mechanism employed by modern serine proteases may be among the most effective.

REFERENCES AND NOTES

1. C. N. Cronin, B. A. Malcolm, J. F. Kirsch, *J. Am. Chem. Soc.* **109**, 2222 (1987).
2. D. L. Sloan, R. Leung, C. S. Craik, E. Sigal, *Nature* **354**, 149 (1991).
3. L. Hedstrom, L. Szilagyi, W. J. Rutter, *Science* **255**, 1249 (1992).
4. R. Bone, J. L. Silen, D. A. Agard, *Nature* **339**, 191 (1989).
5. L. Abrahmsen *et al.*, *Biochemistry* **30**, 4151 (1991).
6. R. A. Lerner, S. J. Benkovic, P. G. Schultz, *Science* **252**, 659 (1991).
7. For the three-dimensional structure of a hydrolytic antibody without a bound transition state analog see B. Golinelli-Pimpaneau *et al.* [*Structure* **2**, 175 (1994)]. For a computer model structure of a hydrolytic antibody see V. A. Roberts *et al.* [*J. Mol. Biol.* **235**, 1098 (1994)].
8. D. M. Segal *et al.*, *Proc. Natl. Acad. Sci. U.S.A.* **71**, 4298 (1974).
9. S. J. Pollack and P. G. Schultz, *Cold Spring Harbor Symp. Quant. Biol.* **52**, 97 (1987).
10. M. R. Haynes, E. A. Stura, D. Hilvert, I. A. Wilson, *Science* **263**, 646 (1994).
11. J. Guo, W. Huang, T. S. Scanlan, *J. Am. Chem. Soc.* **116**, 6062 (1994). With the use of a labeled norleucine phenylamide substrate, we have measured amidase activity for 17E8 (T. S. Scanlan *et al.*, in preparation).
12. A. Tramontano, K. D. Janda, R. A. Lerner, *Science* **234**, 1566 (1986).
13. S. J. Pollack, J. W. Jacobs, P. G. Schultz, *ibid.*, p. 1570.
14. The rate acceleration value of 2.2×10^4 is lower than might be expected on the basis of the high value of k_{cat}. This result is due to the background reaction being substantially accelerated by hydroxide at pH 9.5 where the antibody is most active.
15. In partitioning experiments with hydroxylamine, an antibody-acyl intermediate is trapped as the hydroxamic acid. The amount of the hydroxamate product formed increases with increasing hydroxylamine concentration, whereas the rate of catalytic turnover as measured by phenol release is unaffected by hydroxylamine. This partitioning behavior supports a mechanism of hydrolysis that involves rate-limiting formation of an acyl-antibody intermediate followed by rapid deacylation.
16. E. Harlow and D. Lane, *Antibodies: A Laboratory Manual* (Cold Spring Harbor Press, Cold Spring Harbor, NY, 1988).
17. J. Janarik and S. H. Kim, *J. Appl. Crystallogr.* **24**, 409 (1991).
18. M. B. Lascombe *et al.*, *Proc. Natl. Acad. Sci. U.S.A.* **86**, 607 (1989).
19. A. T. Brünger, D. J. Leahy, T. R. Hynes, R. O. Fox, *J. Mol. Biol.* **221**, 239 (1991).
20. A. T. Brünger, *X-PLOR Manual, Version 3.1* (Yale Univ. Press, New Haven, CT, 1992).
21. Starting with the search model, for the top 1000 orientation angles from rotation function (RF) search, rigid-body Patterson correlation (PC) refinement with independent variable and constant domains, and with independent V_H, V_L, C_H1, C_L (V, variable; C, constant) domains were carried out sequentially for every potential solution. A single angle set representing the possible orientation of the model was identified after this PC refinement. This peak is the ninth in the RF search. Translation searches were carried out with two different space groups, $P2$ and $P2_1$. No solutions were observed in space group $P2$. A convincing correlation (20 σ) was observed for a single position in space group $P2_1$. This confirms that the 17E8 space group is $P2_1$. The R factor for this solution was 0.41 between 6.0 to 2.5 Å. Subsequent structure refinement with X-PLOR included rigid body refinement, additional rigid body refinement with independent variable and constant domains, further rigid body refinement with independent V_H, V_L, C_H1, C_L domains, and Powell minimization. At this point, the R_{cryst} value was 0.38. A slow-cool refinement consisting of 80 steps Cα-restrained conjugate gradient minimization, and subsequent molecular dynamics starting at 3000 K and ending at 300 K over 2.7 picoseconds, followed by 120 steps of conjugate gradient minimization lowered the R factor to 0.207 between 6 to 2.5 Å resolution with rms deviations of bond lengths and bond angles from ideality of 0.020 and 4.3, respectively.
22. E. A. Kabat, T. T. Wu, H. M. Perry, K. S. Gottesman, C. Foeller, *Sequences of Proteins of Immunological Interest* (U.S. Department of Health and Human Services, Washington, DC, 1991).
23. S. Blackburn, *Enzyme Structure and Function* (Dekker, New York, 1976).
24. A. Fersht, *Enzyme Structure and Mechanism* (Freeman, New York, 1985).
25. The closest approach of the Ser^{H99} hydroxyl hydrogen is 2.6 Å to the oxygen atom of Tyr^{H101}.
26. R. M. Stroud, L. M. Kay, R. E. Dickerson, *Cold Spring Harbor Symp. Quant. Biol.* **36**, 125 (1974).
27. M. Krieger, L. M. Kay, R. M. Stroud, *J. Mol. Biol.* **83**, 209 (1974).
28. A. A. Kossiakoff, F. A. Jurnak, A. McPherson, Eds., *Biological Macromolecules and Assemblies* (Wiley, New York, 1987), vol. 3.
29. R. M. Stroud, *Am. Sci.* **231**, 74 (1974).
30. C. S. Craik *et al.*, *Science* **228**, 291 (1985).
31. S. Sprang *et al.*, *ibid.* **237**, 905 (1987).
32. C. S. Craik, S. Roczniak, C. Largman, W. J. Rutter, *ibid.*, p. 909.
33. P. Carter and J. A. Wells, *Nature* **332**, 564 (1988).
34. D. R. Corey and C. S. Craik, *J. Am. Chem. Soc.* **114**, 1784 (1992).
35. D. R. Corey, M. E. McGrath, J. R. Vasquez, R. J. Fletterick, C. S. Craik, *ibid.*, p. 4905.
36. Table 3 compares effects on turnover number (k_{cat}) that result from certain mutations that alter the catalytic triad of serine proteases with the use of available values. It is not our intention to compare directly the turnover number of the catalytic antibody 17E8 with those of wild-type and mutant serine proteases because the kinetic values were obtained with different substrates with varying intrinsic reactivity.
37. Y. Tang, J. B. Hicks, D. Hilvert, *Proc. Natl. Acad. Sci. U.S.A.* **88**, 8784 (1991).
38. S. A. Lesley, P. A. Patten, P. G. Schultz, *ibid.* **90**, 1160 (1993).
39. S. S. Husain and G. Lowe, *Biochem J.* **108**, 855 (1968).
40. F. A. Johnson, S. D. Lewis, J. A. Shafer, *Biochemistry* **20**, 44 (1981).
41. ———, *ibid.*, p. 48.
42. ———, *ibid.*, p. 52.

43. Supported by the American Cancer Society research grant BE-140 (T.S.S.); NIH grant DK39304 (R.J.F.); a postdoctoral fellowship from the American Heart Association–California Affiliate (G.W.Z.); and the Council on Tobacco Research (grant 248). We thank N. Buckley, P. Schultz, R. Lerner, and M. Pique for helpful discussions. The coordinates for 17E8 have been deposited in the Brookhaven Protein Data Bank.

31 March 1994; accepted 12 July 1994